Fast secondary dynamics for enhanced charge transport in polymerized ionic liquids

Z. Wojnarowska,[1,*] M. Musiał,[1] S. Cheng,[1] E. Drockenmuller,[2] and M. Paluch[1]

[1]*Institute of Physics, the University of Silesia in Katowice, Silesian Center for Education and Interdisciplinary Research, 75 Pulku Piechoty 1A, 41–500 Chorzow, Poland*

[2]*Université Lyon, Université Lyon 1, CNRS, Ingénierie des Matériaux Polymères UMR 5223, F-69003 Lyon, France*

(Received 19 September 2019; accepted 21 February 2020; published 18 March 2020)

Segmental dynamics is considered as a major factor governing ionic conductivity of polymerized ionic liquids (PILs), envisioned as potential electrolytes in fuel cells and batteries. Our dielectric studies performed in *T-P* thermodynamic space on ionene, composed of the positively charged polymer backbone and freely moving anions, indicate that other relaxation modes, completely ignored so far, can affect the charge transport in PILs as well. We found that fast mobility manifested by a secondary β process promotes segmental dynamics and thereby increases ionic conductivity making the studied material a first coupled PIL of superionic properties. The molecular mechanism underlying such a β process has been identified as Johari-Goldstein relaxation giving experimental proof that fast secondary relaxations of intermolecular origin exist also in PILs and thereby reveal a universal character.

DOI: 10.1103/PhysRevE.101.032606

I. INTRODUCTION

Although being a relatively new class of materials, polymerized ionic liquids have already shown great potential in the fields of materials sciences and modern technologies [1–3]. The constantly growing attention from the academic and industrial communities comes from their multiple applications as sorbents [4], dispersants [5], carbon precursors [6], and solid electrolytes in various electrochemical devices, such as supercapacitors, batteries, fuel cells, and solar cells [7–9]. Since most high–performance polymerized ionic liquids (PILs) exist as viscous liquids or amorphous solids, at ambient conditions the leakage and safety issues often appearing for conventional ionic liquid-based devices can be easily overcome. However, one of the critical hurdles toward the commercialization of PIL-based electrolytes is their insufficient ionic conductivity (σ_{dc}) at ambient temperature [10]. Thus, understanding fundamental parameters controlling this crucial applicative property is critical for widespread applications of PILs [11–13].

According to the classical picture, ion transport in PILs is governed by the segmental mobility of polymer chains [14]. Thus, a classical strategy to enhance ionic conductivity at ambient conditions is to design derivatives with lower glass transition temperature, T_g [15]. This is because a decrease of T_g makes the segmental dynamics faster and thereby rises ionic conductivity at ambient conditions. A recent alternative relies on the synthesis of PILs with charge transport being independent of segmental mobility [16,17]. Nevertheless, relaxation dynamics on the time scale shorter than segmental motions have never been considered as a promising direction for the development of highly conductive PILs. In this context, fast intermolecular motions regarded as a precursor of slow segmental dynamics seems to be of fundamental importance [18]. Such a local relaxation, considered as a universal and intrinsic feature of supercooled and glassy states, was found to reveal a broad connection to various properties of amorphous solids (e.g., mechanical, thermal stability, or crystallization) [19,20]. However, at the same time, it has never been observed for PILs, since the dielectric reports on PILs are limited to supercooled and normal liquid states.

Herein, we employ dielectric spectroscopy to investigate the dynamics at different length scales of PIL having main-chain 3-methyl-1,2,3-triazolium (TAZ^+) based cations and freely moving bis(trifluoromethylsulfonyl)imide ($TFSI^-$) counter-anions (TPIL), the single-ion conductor of particularly high ionic conductivity (i.e., $\sigma_{dc} = 1.6 \times 10^{-5}$ S cm^{-1}) under anhydrous conditions [21]. We found that ion transport of TPIL is coupled to segmental α process at $T > T_g$, and two fast relaxations, β and γ exist both in the supercooled and the glassy region. The measurements under high-pressure conditions up to 650 MPa revealed a strong correlation between β-mode and ionic conductivity relaxation confirming the existence of the Johari-Goldstein (JG) process in PIL and suggesting that fast dynamics can be a general and unprecedented approach to enhance charge transport in ionic polymers. Finally, it is shown that TPIL becomes superionic conducting polymer due to the β mode.

II. EXPERIMENTAL

A. Material

TPIL studied herein was synthesized as described earlier in two steps comprising AB+AB CuAAC polyaddition of a triethylene glycol-based α-azide-ω-alkyne monomer and subsequent *N*-alkylation of the 1,2,3-triazole groups, and introduction of the bis(trifluoromethylsulfonyl)imide

*Corresponding author: zaneta.wojnarowska@smcebi.edu.pl

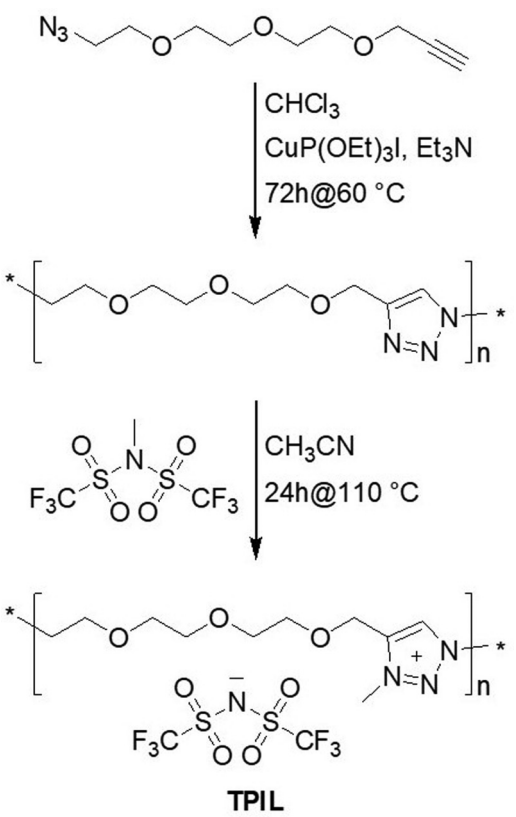

FIG. 1. Two-step synthesis of TPIL by CuAAC polyaddition and *N*-alkylation of the resulting poly(1,2,3-triazole) with CH_3TFSI.

counteranions in a single step using *N*-methyl bis(trifluoromethylsulfonyl)imide (CH_3TFSI) (see Fig. 1) [22,23]. Prior to the measurements TPIL was dried at 383 K under vacuum for 24 h.

B. Temperature-modulated differential scanning calorimetry (TMDSC)

Calorimetric experiments of TPIL were performed using a Mettler Toledo DSC1 STAR System equipped with a liquid nitrogen cooling accessory and an HSS8 ceramic sensor (a heat flux sensor with 120 thermocouples). Using a stochastic TMDSC technique, the dynamic behavior of the liquid-glass transition of TPIL was analyzed in the frequency range from 4 to 40 mHz in a single measurement at a heating rate of 0.5 K min^{-1}. In these experiments, the temperature amplitude of the pulses of 0.5 K was selected. The calorimetric structural relaxation times $\tau_\alpha = 1/2\pi f$ have been determined from the temperature dependences of the real part of the complex heat capacity $c'_p(T)$ obtained at different frequencies in the glass transition region. The glass transition temperature (T_g) was determined for each frequency as the temperature of the half-step height of $c'_p(T)$.

C. Broadband dielectric spectroscopy (BDS) at ambient and elevated pressures

Isobaric dielectric measurements at ambient pressure at frequencies ranging from 10^{-2} to 10^6 Hz were carried out using a Novocontrol GMBH α dielectric spectrometer. For the isobaric measurements, the sample was placed between two stainless steel electrodes of the capacitor with a gap of 0.1 mm. The dielectric spectra of TPIL were collected over a wide temperature range. The temperature was controlled by the Novo-Control Quattro system, with the use of a nitrogen gas cryostat. Temperature stability of the samples was better than 0.1 K. For the pressure dependent dielectric measurements we used a capacitor, filled with the examined sample, which was next placed in the high-pressure chamber and compressed using silicone oil. Note that during the measurement the sample was in contact with stainless steel and Teflon. Pressure was measured by the Unipress setup with a resolution of 0.1 MPa. The temperature was controlled within 0.1 K by means of a Weiss fridge.

D. Rheological measurements

The viscoelastic properties of TPIL were measured by means of an ARES G2 Rheometer. The shear modulus measurements were performed by means of an aluminum parallel plates geometry (diameter = 8 mm). The investigated samples were tested in the frequency range from 0.1 to 100 rad s^{-1} (12 points per decade) and over the temperature range from 246 to 288 K.

III. RESULTS AND DISCUSSION

The dielectric response of TPIL was measured over a broad range of frequency ($f = 10^{-2}-10^6$ Hz) and temperature ($T = 138-288$ K) by means of a Novocontrol α analyzer. Since only the electric modulus representation $M^*(f) = 1/\varepsilon^*(f)$ gives the possibility of investigating the relaxation dynamics of PILs in both supercooled and glassy states [24], we have employed this formalism to analyze the dielectric data of TPIL (Fig. 2). Above the liquid-glass transition the imaginary part of $M^*(f)$ [i.e., $M''(f)$] exhibits a well-pronounced maximum defining the conductivity relaxation time, $\tau_\sigma = 1/2\pi f_{max}$, which corresponds to the mean rate required for ion hopping at a given temperature [25]. On the other hand, below T_g, when the ion hopping is negligible, two distinct loss peaks, labeled as β and γ relaxations, are resolved in the frequency dispersion of M''. Both fast secondary relaxation processes are also well visible on the masterplot (see inset to Fig. 2) constructed by superimposing a number of $M''(f)$ curves measured at different T conditions to the reference spectrum recorded at 242 K. From inset to Fig. 2 it is also evident that the shape of the σ relaxation is practically T invariant and well described by means of a Fourier transform of the Kohlrausch-Williams-Watts (KWW) function:

$$\varphi(t) = \exp[-(t/\tau_\sigma)^{\beta_{KWW}}], \quad (1)$$

with the β_{KWW} exponent equal to 0.55.

To provide a more detailed characterization of ion dynamics in TPIL at $T > T_g$ the conductivity relaxation times τ_σ have been plotted in log scale as a function of inverse temperature. The non-Arrhenius T dependence of τ_σ, quantified by means of the fragility index $m_p = \frac{d\ \log\tau_\sigma}{dT_g/T}$ equal to 123 ± 8, is shown in Fig. 3(a). This relatively steep T dependence of ion dynamics, reflecting one of the most fragile nature among PILs as well as conventional polymers reported so far [26], is

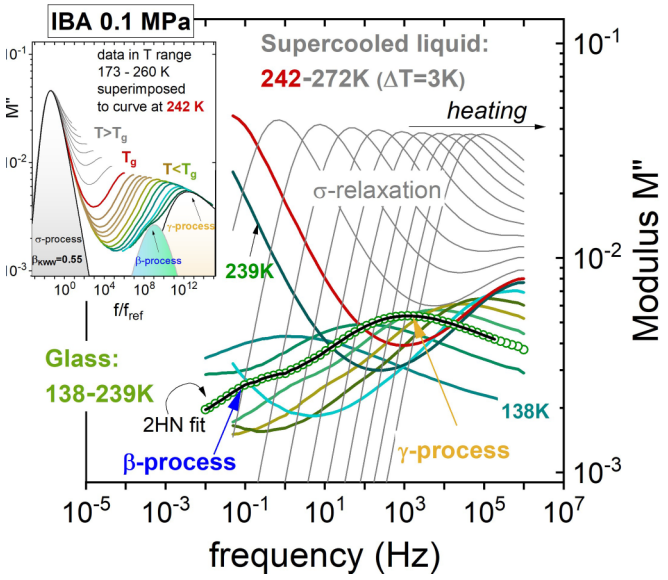

FIG. 2. The representative dielectric spectra of TPIL presented in modulus formalism. Inset: The electric modulus spectra of TPIL recorded at 0.1 MPa and various temperatures superimposed to the spectrum collected at 242 K. Black line indicates the fit of KWW function to conductivity relaxation peak.

most likely due to the polar triethylene glycol-TAZ^+ segments of TPIL. This is because polar groups directly attached to the polymer backbone were found to make the dynamics more sensitive to T changes in nonionic macromolecules [27].

Going further, at a certain temperature the characteristic crossover of $\tau_\sigma(T^{-1})$ occurs. Such a Vogel-Fulcher-Tammann (VFT)-Arrhenius transition is usually identified with the vitrification phenomenon. Since $T^{\text{cross}} = 238.5\,\text{K}$ and $T_g^{\text{DSC}} = 245\,\text{K}$ the same is true in studied TPIL. Additionally, the change of $\tau_\sigma(T^{-1})$ behavior emerges at $\tau_\sigma = 100\,\text{s}$, i.e., at the time scale commonly identified as the freezing point of cooperative dynamics [28]. Thus, one can assume that the mean ion hopping rates in TPIL agree well with those of the segmental dynamics. To verify this statement rheological (RH) and TMDSC measurements have been performed [see experimental details and Fig. 3(b) for a mastercurve constructed from mechanical $G'(\omega)$ and $G''(\omega)$ data]. The T dependences of segmental relaxation times $\tau_s(T^{-1})$ taken: (i) directly as the inverse of shear modulus peak maxima $G''(\omega)$ and (ii) determined from the real part of complex heat capacity, $c_p'(f)$ are displayed in Fig. 3(a). As clearly seen there is a near coincidence between BDS, TMDSC, and RH results, clearly demonstrating that segmental dynamics fully controls charge transport in TPIL. The same conclusion can be drawn from the Walden plot [29] constructed by using molar conductivity Λ and fluidity data η^{-1}. As clearly seen in Fig. 3(c), the experimental points of TPIL reveal the slope close to unity ($s = 0.95$), i.e., typical for coupled systems having ion transport dominated by viscosity. This is most likely due to the high flexibility of the triethylene glycol-based polymer backbone that limits the free volume required for fast ion transport. However, what is surprising, at the same time the Walden line of TPIL falls above the reference obtained for dilute KCl electrolyte, i.e., it is located in the superionic

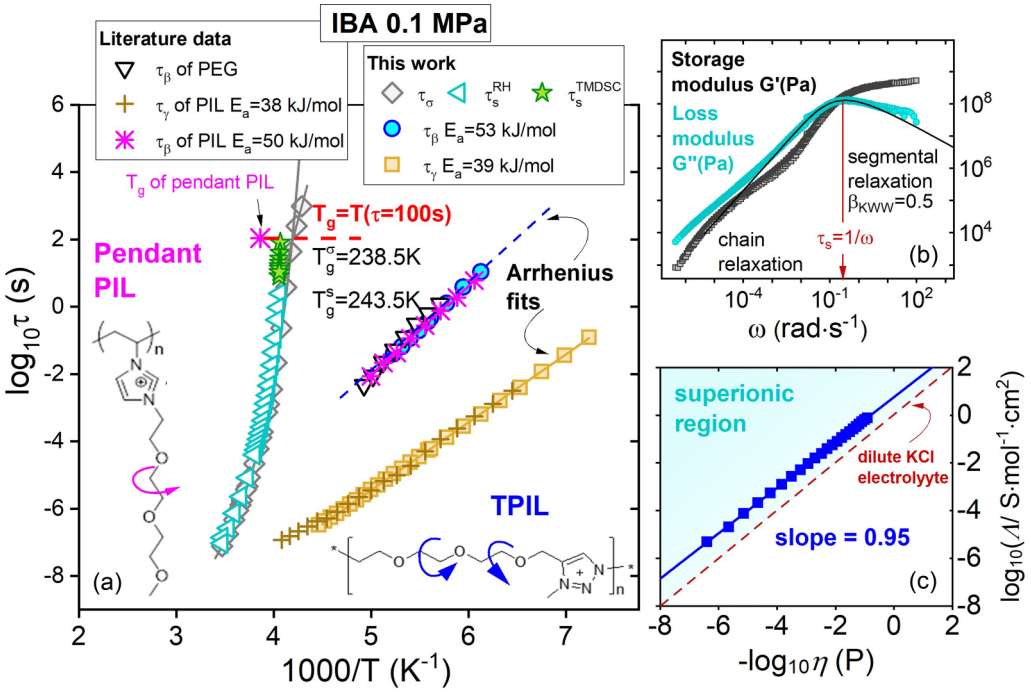

FIG. 3. (a) The relaxation map of TPIL updated by literature results. Solid lines are the VFT (above T_g) and Arrhenius (below T_g) fits of dielectric experimental data. The fragility values are equal to: $m_p^{BDS} = 123 \pm 8$, $m_p^{RH} = 165 \pm 5$. (b) The $G''(\omega)$ and $G'(\omega)$ data of TPIL presented in the form of mastercurve. Solid lines present fit of KWW function to $G''(\omega)$ with $\beta_{\text{KWW}} = 0.5$. (c) Walden plot of TPIL. The η data were taken from Maxwell relation $\eta = \tau_s G^\infty$, while Λ was calculated as $\Lambda = \varepsilon_0 \varepsilon s M/\rho\tau_\sigma$, where M denotes molecular mass and ρ is density taken from Ref. [40].

region, so far available only for decoupled ionic conductors (mostly protic ILs with Grotthuss conduction [30], or PIL with rigid polymer chain [31]). According to the definition Walden plot scales the conducting properties of materials to the same number of ions ($N = 1$ mole). Thus, high molar conductivity $\Lambda = \sigma_{dc}/c = N\mu V/N = \mu V$ of TPIL can be only due to some additional mobility of ions (μ) in a defined volume (V). As a potential source of such extra mobility fast dynamics of cations, being an inherent part of the polymer chain, can be considered. In other words, the existence of the local dynamics promoting the segmental motions and thereby giving a contribution to the overall conductivity of TPIL is expected. To verify this idea a detailed analysis of secondary relaxations observed in dielectric spectra of TPIL needs to be performed.

As mentioned above, the dielectric response of TPIL is characterized by two secondary modes, β and γ, being faster than conductivity relaxation. From the numerical fitting analysis of $M''(f)$ spectra recorded at $T < T_g$ in terms of a combination of two Havriliak-Negami (HN) functions,

$$M^* = \frac{1}{\varepsilon^*} = \left[\varepsilon_\infty + \frac{\Delta\varepsilon}{(1 + (i\varpi\tau)^{\alpha_{NH}})^{\gamma_{HN}}}\right]^{-1}, \qquad (2)$$

where $\Delta\varepsilon$ is the dielectric strength while α_{HN} and γ_{HN} denote $M''(f)$ shape parameters, the time scale of both these processes has been determined precisely at various T conditions (see Fig. 2 for exemplary fit reproducing the dielectric data). The Arrhenius T dependences of τ_β and τ_γ are shown in Fig. 3(a) together with the value of the activation energy barrier determined for each mode. Interestingly, glassy dynamics of the same characteristic was reported earlier for other PIL having triethylene glycol side chains [poly(*N*-vinyl diethylene glycol ethyl methyl ether imidazolium bis(trifluoromethylsulfonyl)imide) PEGVIm-TFSI] [32]. From the comparison presented in Fig. 3(a), it is evident that the absolute value of relaxation times and the activation energy barrier of β and γ processes are practically the same for both derivatives. To identify the molecular origin of observed fast relaxations one needs to look closer on the chemical structure of these polycations since motions within counterions (i.e., TFSI) require very low energy. The joint feature of TPIL and PEGVIm-TFSI is the triethylene glycol (TEG) group directly attached to heterocyclic cation (1,2,3-triazolium *vs* imidazolium). Since conformational changes within both these moieties bring a variation of dipole moment they can be considered as a potential source of fast modes observed in dielectric spectra of TPIL and PEGVIm-TFSI. Quantum chemical calculations have shown that the imidazolium ring can easily rotate with an energy barrier of ca. 30 kJ/mol [33]. Thus, it is reasonable to assign the γ processes of TPIL and PEGVIm-TFSI to the fast rotational motions of the heterocyclic cations. On the other hand, β relaxation can be identified with conformational changes within TEG moiety. The latter suggestion is strongly supported by dielectric data of pure poly(ethylene glycol) (PEG) [34] inserted in Fig. 3(a). Amazingly, regardless of the different ionicity of macromolecule (neutral PEG vs charged PILs) and location within the polymer microstructure (main-chain vs side-chain) dynamics of the TEG group appears as a fast β mode characterized by a fixed position on the relaxation map. With this finding in mind, one can ask, whether or not the fast dynamics expressed as the β process, is coupled to segmental relaxation and consequently affects charge transport of PILs? The answer to this fundamental question can be gained by testing the pressure sensitivity of fast processes in relation to the segmental one. In general, isothermal compression up to 500 MPa, leading to the density change of around 10%, should affect motions of intermolecular origin (treated as a precursor of slower cooperative dynamic), and does not influence the fast dynamics of intramolecular origin [35,36].

The evolution of loss modulus spectra registered during isothermal compression of TPIL at 273 K is presented in Fig. 4(a). In analogy to isobaric compression, squeezing of the studied material leads to the formation of the glassy state with two secondary processes visible in the dielectric window. However, the pressure sensitivity of the β mode is significantly larger than that of the faster γ process. Consequently, β relaxation becomes well separated from the γ process at elevated pressures. Similar results have been obtained for two other isotherms at 263 and 253 K [see Fig. 4(b)] Additionally, at a fixed value of τ_σ (above T_g) or τ_β (below T_g) the dispersion of σ and β processes is independent of thermodynamic conditions (T and P). The closer inspection of obtained high-pressure dielectric data with the same analytical protocol as before gives the pressure dependence of τ_σ, τ_β, and τ_γ displayed in Fig. 4(c). An important feature shared by all $\tau_\sigma(P)$ dependences is the VFT-Arrhenius crossover, occurring at $\tau_\sigma = 100$ s, i.e., just as for ambient pressure $\tau_\sigma(T^{-1})$ data, however this time indicating the glass-transition pressure, P_g. Additionally, it is evident that each pressure evolution of conductivity relaxation times is accompanied by an increase of τ_β, while τ_γ remains constant. To quantify this effect the activation volume parameter ΔV, defined as the volume required to start a dynamic process, has been determined for fast β mode as well as for slower σ relaxation [37]:

$$\Delta V = 2.303\mathrm{RT}\left(\frac{\partial \log\tau}{\partial \mathrm{P}}\right). \qquad (3)$$

As illustrated in Fig. 4(e), ΔV^β decreases with heating, similarly as the ΔV^σ does [see Fig. 4(d)]; however, over the same T range, the change of ΔV^σ is much more pronounced. On the other hand, when the isobaric conditions (IBA 0.1 MPa vs 420 MPa) are considered activation energy barrier of the β process is practically the same [see Fig. 5(a)] and the $\tau_\beta(T^{-1})^{420\,\mathrm{MPa}}$ data perfectly scale with $\tau_\beta(T^{-1})^{0.1\,\mathrm{MPa}}$ when plotted as a function of T/T_g [see Fig. 5(b)]. This result indicates that fast motions within TEG moiety, being an inherent part of the polymer backbone, can be regarded as a true precursor of conductivity relaxation, and because of coupling between τ_s and τ_σ also true precursor of segmental dynamics. This statement can be additionally corroborated by using the coupling model (CM) [38]:

$$\tau_0(T, P) = (t_c)^{1-\beta_{\mathrm{KWW}}}[\tau_\sigma(T, P)]^{\beta_{\mathrm{KWW}}}. \qquad (4)$$

According to this formula, a direct connection of secondary mode with conductivity relaxation τ_σ occurs when equality between τ_β and primitive relaxation time τ_0 is nearly satisfied.

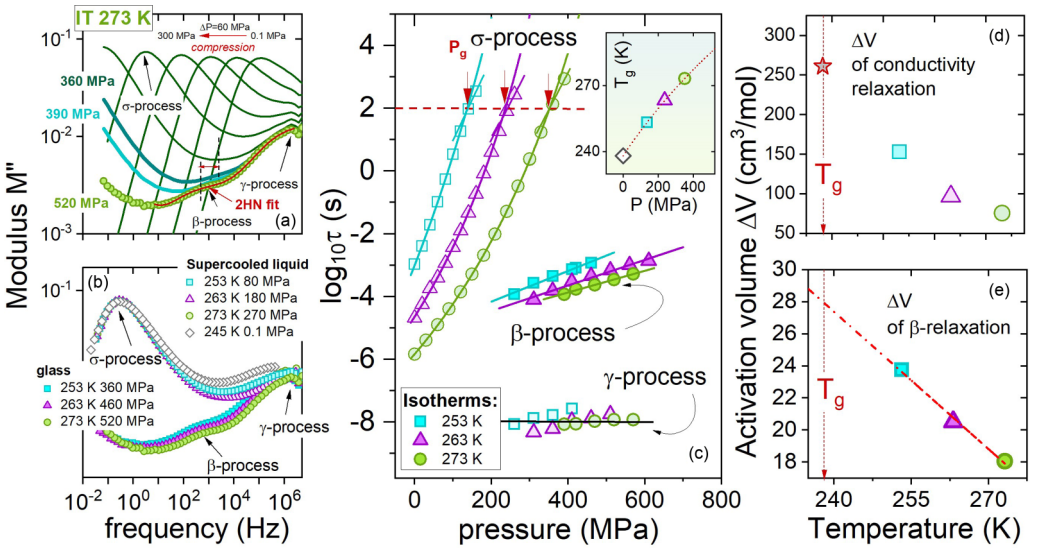

FIG. 4. High-pressure data for TPIL. (a) The isothermal dielectric measurements collected at 273 K and 0.1–520 MPa pressure range; (b) The representative $M''(f)$ peaks recorded at various T-P conditions; (c) Isothermal dependences of τ_σ, τ_β, and τ_γ; Benefiting from crossover of $\tau_\sigma(P)$ we have constructed the $T_g(P_g)$ plot [see inset panel (c)] and determined the pressure coefficient of glass transition temperature ($dT_g/dP = 110$ K/GPa); (d). Activation volume of conductivity relaxation calculated from Eq. (3) in the limit of ambient pressure. The value of ΔV^σ at T_g was calculated as $\Delta V^\sigma = 2.303R(dT_g/dP)m_P$; (e) Activation volume of β relaxation calculated from Eq. (3) in the limit of ambient pressure.

Then, the intermolecular nature of secondary relaxation is proved and the mode is coined as the JG process [39]. As illustrated in Fig. 5(a), the relaxation times of a fast β process stay in good agreement with CM predictions obtained from parameters describing width and temperature behavior of the $M''(f)$ peak, i.e., $\beta_{KWW} = 0.55$. Additionally, exactly the same results are obtained when the quantities characterizing real segmental relaxation are used [$\beta_{KWW} = 0.5$ and $\tau_s(T)$, see Fig. 5(b)].

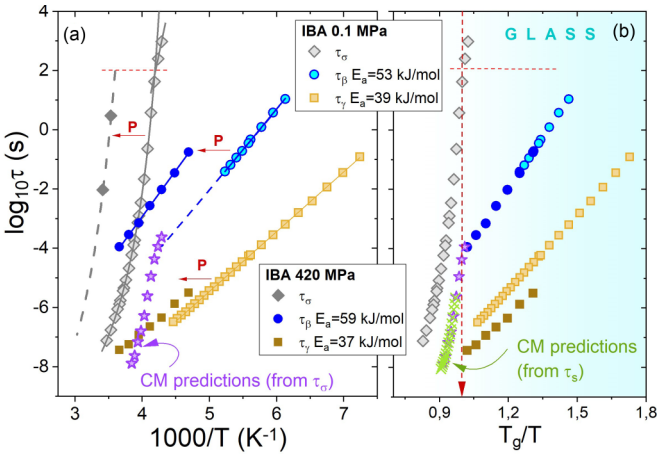

FIG. 5. (a) Relaxation map of TPIL constructed from ambient and high-pressure data. Violet stars present τ_0 determined from CM by using ambient pressure τ_σ data [Eq. (4)]; (b) T_g/T dependence of TPIL relaxation times. Violet stars present τ_0 determined from CM by using ambient pressure τ_σ data [Eq. (4)], while green crosses are τ_0 determined from CM by us ambient pressure τ_s data. The value of T_g at 420 MPa used to scale high-pressure $\tau_\beta(T^{-1})$ and $\tau_\gamma(T^{-1})$ dependences was determined from $T_g(P_g)$ dependence presented in the inset to Fig. 4(c).

Interestingly, in contrast to TPIL having a main-chain TEG group, the fast motions of pendant-TEG groups of PEGVIm-TFSI visible as the β process, were found to be insensitive to density changes and have no effect on segmental dynamics and charge transport [32]. Thus, in contrast to TPIL, no additional contribution from fast dynamics to ion conductivity can be expected. In this way, TPIL can be considered as the first ionic polymer for which the JG β relaxation, being strongly connected to segmental dynamics and thus promoting charge transport, has been observed and confirmed.

IV. CONCLUSIONS

In summary, we have investigated the molecular dynamics of a 1,2,3-triazolium-based polymerized ionic liquid in both the supercooled region and the glassy state. At $T > T_g$ TPIL is characterized by ion transport strongly coupled to the segmental α process (as determined from mechanical measurements), while two fast secondary relaxations (β and γ) appear in the dielectric spectra of supercooled and glassy state. The β mode, reflecting the motions of the main chain TEG groups, satisfies coupling model predictions and is sensitive to density changes. Thus, it can be classified as a true precursor of TPIL segmental dynamics and thereby considered an example of JG relaxation in PILs. It has been also recognized as the source of extra mobility responsible for the superionic properties of TPIL. Importantly, fast motions of the side-chain TEG groups, although manifested by the β mode of the same characteristic at ambient pressure, are completely independent of segmental dynamics and thus have no effect on charge transport. Thereby, only the secondary dynamics of intermolecular origin can be specified as an additional factor influencing the dc conductivity of PILs in

addition to chain flexibility, dielectric constant, ion size, and T_g value. This knowledge provides a crucial understanding of dynamics in PILs and thereby offers a general strategy for further designing PILs with enhanced σ_{dc}.

ACKNOWLEDGMENT

The authors are deeply grateful for the financial support by the National Science Centre within the framework of the Opus15 project (Grant No. DEC- 2018/29/B/ST3/00889).

[1] A. Armand, F. Endres, D. R. MacFarlane, H. Ohno, and B. Scrosati, Nat. Mater. **8**, 621 (2009).
[2] D. R. MacFarlane, M. Forsyth, P. C. Howlett, M. Kar, S. Passerini, J. M. Pringle, H. Ohno, M. Watanabe, F. Yan, W. Zheng, S. Zhang, and J. Zhang, Rev. Nat. Mater. **1**, 15005 (2016).
[3] J. Y. Yuan and M. Antonietti, Polymer **52**, 1469 (2011).
[4] A. Wilke, J. Yuan, M. Antonietti, and J. Weber, ACS Macro Lett. **1**, 1028 (2012).
[5] Y. Biswas, T. Maji, M. Dule, and T. K. Mandal, Polymer Chem. **7**, 867 (2016).
[6] S. Cheng, B. Chen, L. Qin, Y. Zhang, G. Gao, and M. He, RSC Adv. **9**, 8137 (2019).
[7] J. M. Tarascon and M. Armand, Nature (London) **414**, 359 (2001).
[8] M. R. Palacín, Chem. Soc. Rev. **38**, 2565 (2009).
[9] M. Forsyth, L. Porcarelli, X. Wang, N. Goujon, and D. Mecerreyes, Acc. Chem. Res. **52**, 686 (2019).
[10] V. Ganesan, Mol. Syst. Des. Eng. **4**, 280 (2019).
[11] Q. Zhao, C. Shen, K. P. Halloran, and C. P. Evans, ACS Macro Lett. **8**, 658 (2019).
[12] J. R. Keith, N. J. Rebello, B. J. Cowen, and V. Ganesan, ACS Macro Lett. **8**, 387 (2019).
[13] A. Pipertzis, M. Mühlinghaus, M. Mezger, U. Scherf, and G. Floudas, Macromolecules **51**, 6440 (2018).
[14] H. Ohno, *Electrochemical Aspects of Ionic Liquids* (Wiley, New York, 2005).
[15] C. A. Angell, Solid State Ionics **9**, 3 (1983).
[16] F. Fan, W. Wang, A. P. Holt, H. Feng, D. Uhrig, X. Lu, T. Hong, Y. Wang, N. -G. Kang, J. Mays, and A. P. Sokolov, Macromolecules **49**, 4557 (2016).
[17] F. Mizuno, J. P. Belieres, N. Kuwata, A. Pradel, M. Ribes, and C. A. Angell, J. Non-Cryst. Solids **352**, 5147 (2006).
[18] C. Leon, K. L. Ngai, and J. Habasaki, *Dynamics of Glassy, Crystalline, and Liquid Ionic Conductors: Experiments, Theories, Simulations* (Springer, New York, 2017).
[19] L. Berthier, E. Flenner, and G. Szamel, J. Chem. Phys. **150**, 200901 (2019).
[20] S. Kolodziej, S. Pawlus, K. L. Ngai, and M. Paluch, Macromolecules **51**, 4435 (2018).
[21] M. M. Obadia and E. Drockenmuller, Chem. Commun. **52**, 2433 (2016).
[22] S. Cheng, Z. Wojnarowska, M. Musiał, D. Flachard, E. Drockenmuller, and M. Paluch, ACS Macro Lett. **8**, 996 (2019).
[23] B. P. Mudraboyina, M. M. Obadia, I. Allaoua, R. Sood, A. Serghei, and E. Drockenmuller, Chem. Mater. **26**, 1720 (2014).
[24] I. M. Hodge, K. L. Ngai, and C. T. Moynihan, J. Non-Cryst. Solids **351**, 104 (2005).
[25] C. Gainaru, E. W. Stacy, V. Bocharova, M. Gobet, A. P. Holt, T. Saito, S. Greenbaum, and A. P. Sokolov, J. Phys. Chem. B **120**, 11074 (2016).
[26] K. Kunal, K.G. Robertson, S. Pawlus, S. F. Hahn, and A. P. Sokolov, Macromolecules **41**, 7232 (2008).
[27] A. L. Agapov, Y. Wang, K. Kunal, C. G. Robertson, and A. P. Sokolov, Macromolecules **45**, 8430 (2012).
[28] Z. Wojnarowska, H. Feng, M. Diaz, A. Ortiz, I. Ortiz, J. Knapik-Kowalczuk, M. Vilas, P. Verdía, E. Tojo, and T. Saito *et al.*, Chem. Mater. **29**, 8082 (2017).
[29] C. Schreiner, S. Zugmann, R. Hartl, and H. J. Gores, J. Chem. Eng. Data **55**, 1784 (2009).
[30] M. Yoshizawa, W. Xu, and C. A. Angell, J. Am. Chem. Soc. **125**, 15411 (2003).
[31] D. Bresser, S. Lyonnard, C. Iojoiu, L. Picarde, and S. Passerini, Mol. Syst. Des. Eng. **4**, 779 (2019).
[32] Z. Wojnarowska, H. Feng, Y. Fu, S. Cheng, R. Kumar, V. N. Novikov, A. Kisliuk, T. Saito, N. Kang, J. Mays, A. P. Sokolov, and V. Bocharova, Macromolecules **50**, 6710 (2017).
[33] A. Gruia, R. Curpan, A. Borota, L. Halip, M. Mracec, and M. Mracec, Rev. Roum. Chim. **59**, 605 (2014).
[34] S. Kalakkunnath, D. S. Kalika, H. Lin, R. D. Raharjo, and B. D. Freeman, Macromolecules **40**, 2773 (2007).
[35] K. L. Ngai and M. Paluch, J. Chem. Phys. **120**, 857 (2004).
[36] G. Floudas, M. Paluch, A. Grzybowski, and K. L. Ngai, *Molecular Dynamics of Glass-Forming Systems: Effects of pressure*, edited by F. Kremer, Advances in Dielectrics (Springer-Verlag, Berlin, Heidelberg, 2011).
[37] M. Paluch, *Dielectric Properties of Ionic Liquids* (Springer, Berlin, 2016).
[38] K. L. Ngai, *Relaxation and Diffusion in Complex Systems* (Springer, Berlin, 2011).
[39] G. P. Johari and M. J. Goldstein, J. Chem. Phys. **53**, 2372 (1970).
[40] S. Cheng, M. Musiał, Z. Wojnarowska, A. Holt, M. C. Roland, E. Drockenmuller, and M. Paluch, J. Phys. Chem. B. **124**, 1240 (2020).